



RESEARCH ARTICLE

Automatic Recognition of Leukemia Cells using Texture Analysis Algorithm

*Yousif Mohamed Y. Abdallah¹, Suha Mohammed²

1. Department of Radiological Science and Medical Imaging, College of Medical Applied Science, Majmaah University, Saudi Arabia
2. Department of Radiology, Yasmine Poly Clinics, Makkah, Saudi Arabia

Manuscript Info**Manuscript History:**

Received: 11 November 2015
Final Accepted: 22 December 2015
Published Online: January 2016

Key words:

Recognition,
Leukemia,
Texture Analysis
Algorithm

***Corresponding Author**

**Yousif Mohamed Y.
Abdallah**

Abstract

A trained laboratory specialist usually scored the detection of leukemia cells by determining the leukemia location and size subjectively (by eyes). This subjective method will add to the 5% tolerance error, which might compromise the whole process of treatment especially in patients with severe conditions. The aim of this study is to increase the edge recognition in leukemia cells images in patients with leukemic disease automatically using L*a*b* color space and K-means clustering. First, we read the microscopic images. We then to convert the images form RGB color space to L*a*b* color space. Then we classify the colors in 'a*b*' space using K-means clustering. Then we label every pixel in the Image using the results from K-means. We then create images that segment the leukemia image by color. Finally, we segment the leukemia cell image into a separate image. The sample of this study was (46 cases) and they showed increase enhancement. This segmentation technique (automatic scoring) and segmented images was adjudicated by trained laboratory specialists as being comparable to other segmentation techniques created with manual editing (subjective scoring). The quantitative results calculated using a measure of percentage match between ground truth and segmentation results. The percentage match (PM) measure was 99.33 (p <0.05) and Corresponding Ratio (CR) was -0.007 p <0.05).

Copy Right, IJAR, 2016., All rights reserved.

Introduction:-

Image segmentation has been a long-standing problem in computer vision. It is a very difficult problem for general images, which may contain effects such as highlights, shadows, transparency, and object occlusion. Segmentation in the domain of medical imaging has some characteristics that make the segmentation task easier and difficult at the same time (Abdallah, et al, 2014). On the one hand, the imaging is narrowly focused on an anatomic region. The imaging context is also well defined. While context may be present to some extent in segmenting general images (e.g., indoor vs. outdoor, city vs. nature, people vs. animals), it is much more precise in a medical imaging task, where the imaging modality, imaging conditions, and the organ identity is known (Abdelwahab, et al, 2014). In addition, the pose variations are limited, and there is usually prior knowledge of the number of tissues and the Region of Interest (ROI) (Abdallah et al, 2015). On the other hand, the images produced in this field are one of the most challenging due to the poor quality of imaging making the anatomical region segmentation from the background very difficult. Often the intensity variations alone are not sufficient to distinguish the foreground from the background, and additional cues are required to isolate ROIs (Abdallah, 2016). Finally, segmentation is often a means to an end in medical imaging. It could be part of a detection process such as tissue detection, or for the purpose of quantification of measures important for diagnosis, such as for example, lesion burden which is the number of pixels/voxels within the lesion regions in the brain (Abdallah and Mohamed, 2015). In general, the information contained in an image modeled in several ways. A simple approach is to record the intensity distribution

within an image via a One-dimensional (1D) histogram and use simple thresholding to obtain the various segments. Several variations on classical histogram thresholding proposed for medical image segmentation that incorporate extended image representation schemes as well as advanced information modeling (Abdallah, 2011). Multi-dimensional histograms formed from the intensity values produced by each of the imaging protocols. It is often the case that several acquisitions are available for the same image. Spatial information: Since intensity histograms do not preserve spatial contiguity of pixels, one variation is to add spatial position (x, y) or (x, y, z) to form a multi-dimensional feature vector incorporating spatial layout. If the medical images are in a time sequence (e.g. moving medical imagery), then time can be added as an additional feature in the representation space (Abdallah and Wagiallah, 2014). Thus, these approaches represent each image pixel as a feature vector in a defined multi-dimensional feature space. The segmentation task can be seen as a combination of two main processes; modeling which is the generation of a representation over a selected feature space (Pinz, 1998). This can be termed the modeling stage. The model components viewed as groups, or clusters in the high-dimensional space (Abdallah and Yousef, 2015). In order to be directly relevant for a segmentation task, the clusters in the model should represent homogeneous regions of the image. In general, the better the image modeling, the better the segmentation produced. Since the number of clusters in the feature space are often unknown, segmentation regarded as an unsupervised clustering task in the high dimensional feature space (Meyer and Fernand, 1994).

Material and Methods:-

This was experimental study conducted to study segmentation of color microscopic leukemia image using colors segmentation filters of MatLab image processing program. The study included Elnileen Medical center of Khartoum and Fadil Specialist Hospital. For leukemia cells images, each image scanned using digitizer scanner then treated by using image-processing technique (MatLab), where the segmentation studied. The scanned images saved in PNG and 600 dpi file format to preserve the quality of the image. We used Color-Based Segmentation Using K-Means Clustering Algorithm to enhance the cardiac images. The steps of segmentation shown in the Fig. 1 as below:

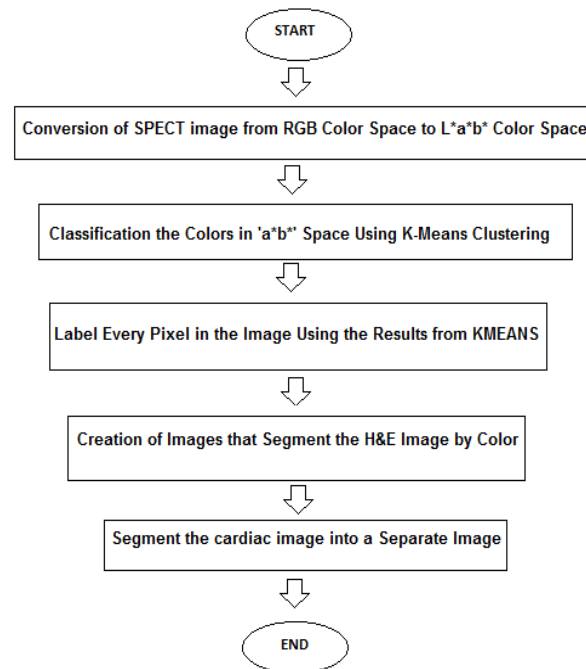


Figure 1. Steps of Colour-Based Segmentation Using K-Means Clustering

Result and Discussion:-

This was experimental study conducted to study segmentation of microscopic leukemia cells image using colours segmentation filters of MatLab image processing program. In this study firstly, we read in SPECT image with extension PNG, which is a colour ischemic heart image. This colour method helps nuclear medicine physician or cardiologist distinguish different heart tissue types Figure 2.

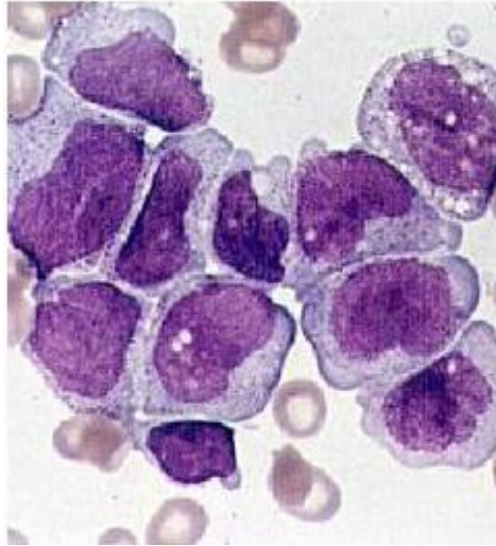


Figure 2. The Original image

Many colours can notice in the cardiac image if one ignore variations in brightness. There are three colors: white, blue, and pink. It is easily to distinguish these colors from one another easily. The $L^*a^*b^*$ color space (also known as CIELAB or CIE $L^*a^*b^*$) enables us to quantify these visual differences. The $L^*a^*b^*$ color space is derived from the CIE XYZ tristimulus values. The $L^*a^*b^*$ space consists of a luminosity layer 'L*', chromaticity-layer 'a*' indicating where color falls along the red-green axis, and chromaticity-layer 'b*' indicating where the color falls along the blue-yellow axis. All of the color information is in the 'a*' and 'b*' layers. We measured the difference between two colors using the Euclidean distance metric. In this study we converted the image to $L^*a^*b^*$ color space using makeform and applyform (forward transformation). The RGB or CMYK values first need to be transformed to a specific absolute color space, such as sRGB or Adobe RGB. This adjustment will be device dependent, but the resulting data from the transform will be device independent, allowing data to be transformed to the CIE 1931 color space and then transformed into $L^*a^*b^*$. The L^* coordinate ranges from 0 to 100. The possible range of a^* and b^* coordinates is independent of the colour space that one is converting from, since the conversion below uses X and Y which come from RGB.

The forward transformation

$$L^* = 116 \left(\frac{Y}{Y_n} \right) - 16 \quad (1)$$

$$a^* = 500 \left[f \left(\frac{X}{X_n} \right) - f \left(\frac{Y}{Y_n} \right) \right] \quad (2)$$

$$b^* = 200 \left[f \left(\frac{Y}{Y_n} \right) - f \left(\frac{Z}{Z_n} \right) \right] \quad (3)$$

Where,

$$f(t) = \begin{cases} t^{1/3} & \text{if } t > \left(\frac{6}{29}\right)^3 \\ \frac{1}{3} \left(\frac{29}{6}\right)^2 t + \frac{4}{29} & \text{otherwise} \end{cases} \quad (4)$$

Where X_n , Y_n and Z_n are the CIE XYZ tristimulus values of the reference white point. The division of the f function into two domains was done to prevent an infinite slope at $t=0$ was assumed to be linear below some $t = t_0$, and was assumed to match the $t^{1/3}$ part of the function at t_0 in both value and slope as shown in Fig.3.

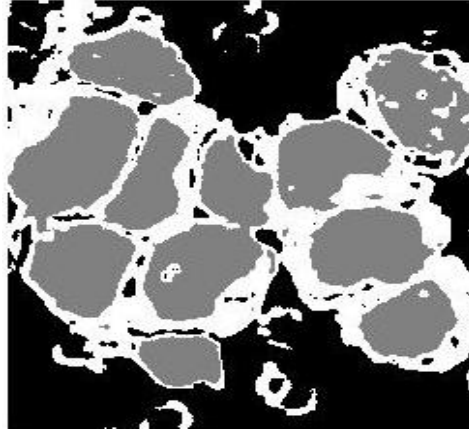


Figure 3. Image Labeled by cluster index

We used K-means clustering in order to treat each object as having a location in space. It found partitions such that objects within each cluster are as close to each other as possible, and as far from objects in other clusters as possible. We specified the number of clusters to be partitioned to 3 and a distance metric to quantify how close two objects in leukemia sample to each other. Since the color information exists in the 'a*b*' space, the objects are pixels with 'a*' and 'b*' values. We used k-means to cluster the objects into three clusters using the Euclidean distance metric as shown in Figure 4.

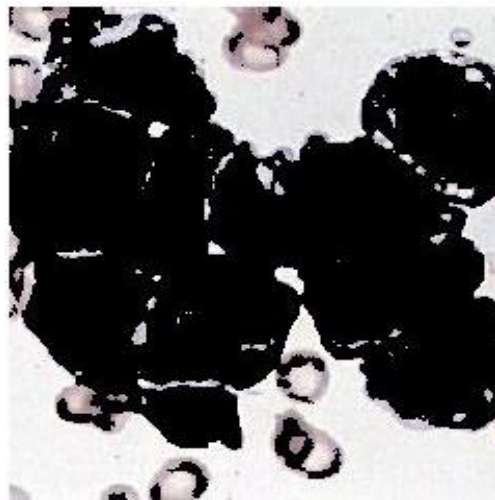


Figure 4. Cluster 1 K-means algorithm

For every structure in our input (microscopic images), k-means returned an index corresponding to a cluster. The cluster_center output from k-means would use later in the demo. Every pixel was label in the image with cluster_index Figure 5.

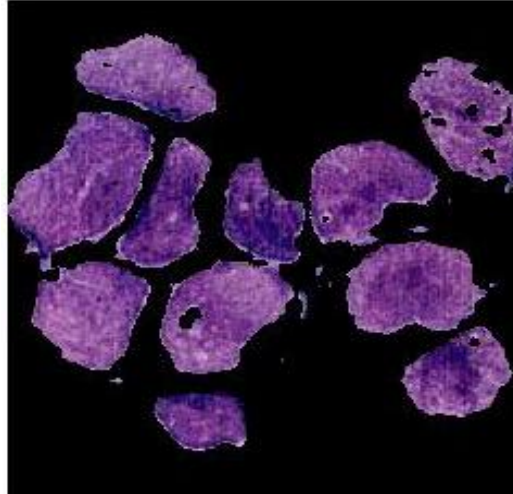


Figure 5. Cluster 2 K-means algorithm

Using pixel_labels, we separated structures in cardiac images by color, which would result in three images Figure 6.

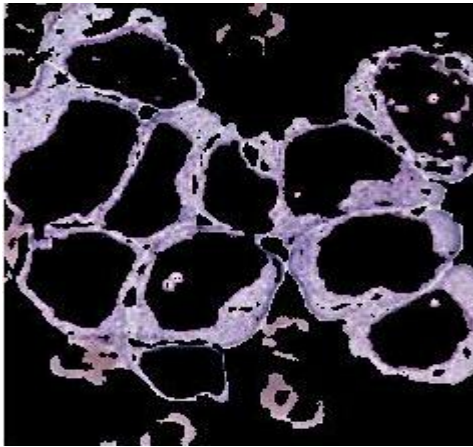


Figure 6. Cluster 2 K-means algorithm

There were dark and light color structures in one of the clusters. We separated dark blue from light blue using the 'L*' layer in the L*a*b* color space. We recalled that the 'L*' layer contains the brightness values of each color. Then we found the cluster that contained the blue objects. We extracted the brightness values of the pixels in this cluster and threshold them using im2bw. We programmatically determined the index of the cluster containing the blue objects because k-means would return the same cluster_idx value every time. We could do this using the cluster_center value, which contains the mean 'a*' and 'b*' value for each cluster. The blue cluster has the smallest cluster_center value (determined experimentally). Finally, We used the mask is_light_blue to label which pixels belong to the cardiac structure. Then We displayed the blue color in a separate image Figure 7.

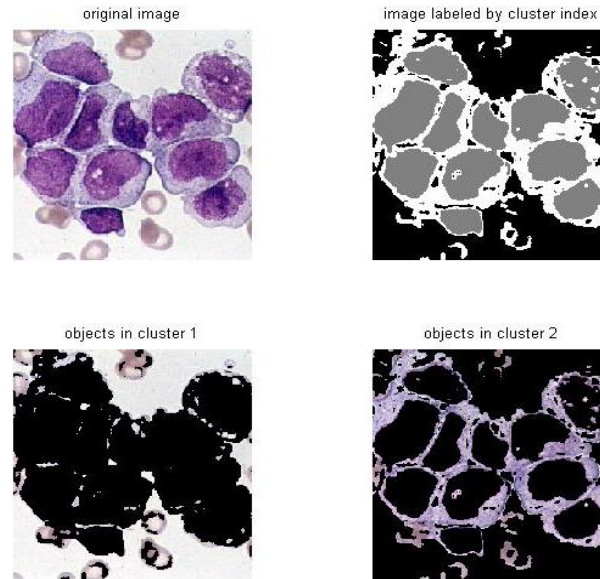


Figure 7. Segmentation of the cardiac images into a Separate Image

References:-

1. **Abdallah, Y., Hayder, A., and Wagiallah ,E., (2014)**, Automatic Enhancement of Mammogram using Contrast Algorithm. *International Journal of Science and Research (IJSR)*,3(9): p. 1886-1891.
2. **Abdelwahab, R., and Abdallah, Y., Hayder, A., and Wagiallah ,E., (2014)**, Application of Texture Analysis Algorithm for Data Extraction in Dental X-Ray Images. *International Journal of Science and Research (IJSR)*,. 3(10): p. 1934-1939.
3. **Abdallah, Y., Alkhir, M., Algaddal, A., (2015)**, Improvement of Brain Tumors Detection Using Markers and Boundaries Transform. *International Journal of Science and Research (IJSR)*,. 4(1): p. 2372-2378.
4. **Abdallah, Y., (2016)**, Increasing of Edges Recognition in Cardiac Scintigraphy for Ischemic Patients. *Journal of Biomedical Engineering and Medical Imaging*, 3(6):p.34-39
5. **Abdallah, Y., (2015)**: An Accurate Liver Segmentation Method Using Parallel Computing Algorithm. *Journal of Biomedical Engineering and Medical Imaging*, 3(2).
6. **Abdallah, Y., Mohamed M., (2015)**, Using Basic Morphology Tools in Improvement of Kidneys Detection. *International Journal of Science and Research (IJSR)*, 4(5):1383-1386.
7. **Abdallah, Y., (2011)**, Application of Analysis Approach in Noise Estimation, Using Image Processing Program. Lambert Publishing Press GmbH & Co. KG, Germany.
8. **Abdallah, Y., and Wagiallah, E., (2014)**, Segmentation of Thyroid Scintigraphy Using Edge Detection and Morphology Filters. *International Journal of Science and Research (IJSR)*, 3(11): p. 2768-2772.
9. **Abdallah, Y., and Hassan, A., (2015)**, Segmentation of Brain in MRI Images Using Watershed-based Technique. *International Journal of Science and Research (IJSR)*, 4(1): p. 683-688.
10. **Pinz, A., (1998)**, Mapping the human retina. *Medical Imaging, IEEE Transactions on*, 1998. 17(4): p. 606-619.
11. **Abdallah, Y., and Yousef R.,(2015)**, Augmentation of X-Rays Images using Pixel Intensity Values Adjustments. *International Journal of Science and Research (IJSR)*, 4(2): p. 2425-2430.
12. **Meyer, Fernand, (1994)**, Topographic distance and watershed lines, *Signal Processing* , Vol. 38, pp. 113-125

